

MODELLING OF SPACE ANTENNA DEPLOYMENT USING OPEN SOURCE SOFTWARE

¹*Institute of Technical Mechanics
of the National Academy of Sciences of Ukraine and the State Space Agency of Ukraine,
15 Leshko-Popel St., Dnipro 49005, Ukraine; e-mail: skh@ukr.net*
²*EOS Ukraine, 31-D Bohdana Khmel'nitskogo Ave., Dnipro, 49055, Ukraine*



The goal of this article is to develop a dynamic model of a space antenna with the pantograph structure and to study the processes of its deployment using open-source software. Methods of theoretical mechanics, multibody dynamics, computational mechanics, and computer modeling were used in the research.

A mesh antenna of the novel design, which is recommended for mini-satellites, is considered as the object for modeling. The most significant difference between this antenna and others is the design of the support ring in the form of a pantograph.

To develop a model of the space antenna dynamics and implement it using open-source software, some simplifications were made due to the complexity of the structure. The antenna model is represented as a system of rigid and flexible bodies connected by hinges. Carbon fiber rods are modeled with the help of a flexible finite element using the method of absolute nodal coordinates, which allows one to model large deformations of the structure. Aluminum hinge assemblies are modeled as several rotation joints connected by conventional rigid elements. The main modeled properties of these hinge assemblies are the stiffness, location, and direction of the axes of rotation of the hinges. The tension forces created by the stretched mesh are modeled using springs. The cable drive of the antenna deployment mechanism is modeled as a load acting on the corresponding elements in defined local positions.

An algorithm for building a model of the space antenna simulate the reflector deployment process in the HotInt open-source software is presented. Using the built model, antenna deployment simulations are carried out for different cases, which differ in the forces used for the deployment. Values of deployment time, variations of angles between the V-folded bars, and tensions in the diagonal rods of the antenna sections during the antenna deployment are obtained.

The approach proposed in the article can be implemented using free software, ensures flexibility of modeling, and reduces the model development time.

Keywords: *reflector antenna, deployment, multibody dynamics, open-source software, flexible beam, joint.*

Introduction. Antennas are used in space for various tasks, such as communi-

cation, military intelligence, remote sensing and climate forecasting. Antennas with a large aperture are used to increase the efficiency of solving such tasks. Due to the fact that the space under the fairing of the launch vehicle is limited, large antennas are designed as transformable structures [1 – 3]. Such structures are launched into orbit in a stowed state, and then in space they are deployed in such a way as to form the desired configuration. Such structures are quite complex, and unfortunately there were cases when such structures were not properly deployed in space. The difficulties in testing the space antenna deployment on Earth encourage engineers and researchers to use computer simulation methods. Modeling such systems is a difficult task, since the deployment of a space antenna reflector is a complex transition from a multibody system with relative motions between its components to a flexible structure.

There is a sufficient number of publications devoted to the problem of modeling the deployment of space antennas, for example [4 – 6]. In most cases, the authors use special computer code of their own development to conduct research. Although such an approach is naturally very flexible, it takes a lot of time to develop and validate this code, because the object of simulation is a complex, multi-element flexible system.

Another approach is to use commercial software for modeling the dynamics of multibody systems, such as Adams [7 – 9] and Ansys Motion [10, 11]. Even though such software has good capabilities, they are still limited by the methodology used when they were created. In addition, these software products are very expensive and inaccessible to startups and small groups of researchers.

Currently, there are a small number of open source software for the simulation of the dynamics of multi body systems, such as MBDyn [12] and Hotint [13]. They are free and may potentially provide modeling flexibility and reduce the time for model development, but unfortunately, there is a lack of publications giving examples of their application for space antenna modeling.

Transformable antennas can have an umbrella [14], truss [15, 16], or mesh [10, 11] design. The last type of antenna is considered the most promising, as they are characterized by a large stowed ratio, high reliability of deployment, small mass, and high stiffness after deployment. The most famous among such structures are the AstroMesh antennas [17] from the Astro Aerospace company. Issues of modeling the deployment of such antennas are reported in Ref. [10, 11]. In papers [10, 11], a new design of mesh antenna was proposed. This antenna design is recommended for mini satellites. A pantograph design of the supporting ring is the most important feature, which differentiates this reflector from the AstroMesh antenna. Such a pantograph structure is considered to be a very promising approach for a reflector design, but there are not any publications about the deployment modeling of such antennas.

The goal of this article is to develop a dynamic model of a space antenna with the pantograph structure and to study the processes of its deployment using open-source software.

Antenna design. Taking into account the comments made above, the antenna proposed in the papers [10, 11] is chosen as the object for this study.

The basis of the antenna design

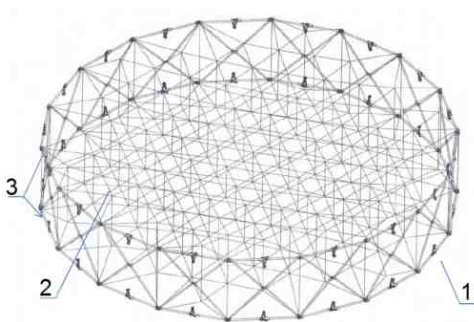


Fig. 1 – Antenna design.

(Fig. 1) is the transformable supporting ring (1). Two nets (2), which are attached to the supporting ring and tensioned by ties and, form the required shape of the reflector. A reflective mesh is attached to one of the nets. The supporting ring of the antenna consists of 18 identical sections connected by hinge units (3). Each section is formed from diagonal and horizontal rods of a tubular cross-section. A fragment of the supporting ring of the antenna is presented in Fig. 2. Figure 3 shows part A of the supporting ring on an enlarged scale.

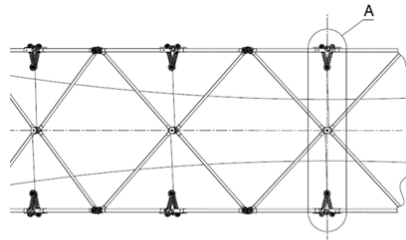


Fig. 2 – Fragment of the supporting ring

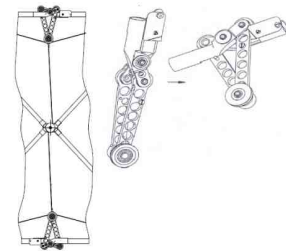


Fig. 3 – V-folding bar hinge

The diagonal rods are connected by hinges, which ensure the rotation of one rod relative to the other. The diagonal rods are also connected to the lower and upper horizontal rods, which are transformable by means of V-folding bar hinges (Fig. 3). The sections of the ring are also connected by hinged units at the junctions of the diagonal and horizontal rods (Fig. 4).

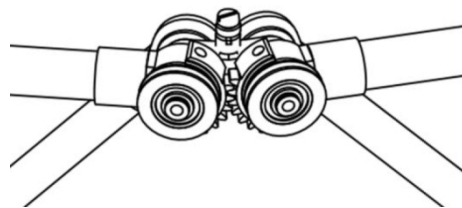


Fig. 4 – Intersectional hinge assembly

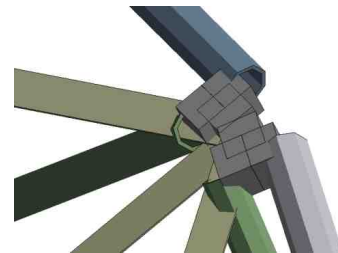


Fig. 5 – Simplified representation of the intersectional hinge assembly

All hinges and connecting elements are made of aluminum, and diagonal and horizontal rods are made of carbon fiber.

The antenna is deployed utilizing cables passing through a system of pulleys and driven by two electric motors.

Antenna model. Due to the complexity of the design of the space antenna, some simplifications were made to create a dynamic model of the deployable structure and its subsequent implementation using open source software.

Carbon fiber rods are modeled by flexible beam elements using based on the absolute nodal coordinate formulation (ANCF) [18]. These finite elements are capable of simulating large deformations and can be used for both static and dynamic studies. They model axial, bending, shear, and torsion deformation of the rods. The ANCF uses slope vectors to parameterize the orientation of the cross-section of the beam instead of the rotation parameters.

The orientation of the cross-section of the beam is described using conventional linear interpolation, and displacements along its axis are interpolated using linear shape functions. The slope vectors are derivative vectors with respect to the

reference frame of the scaled linear base element. The definition of elastic is based on a continuum mechanics-based formulation for a St.Venant Kirchhoff [19] material using the relationship between the nonlinear Green-Lagrange strain tensor and the second Piol-Kirchhoff stress tensor. The degrees of freedom of the i -th node can be given as follows

$$q^{(i)} = \begin{bmatrix} u^{(i)T} & u_{\eta}^{(i)T} & u_{\zeta}^{(i)T} \end{bmatrix}^T, \quad (1)$$

where $u^{(i)}$ is the nodal displacement; $u_{\eta}^{(i)}, u_{\zeta}^{(i)}$ are the changes of the slope vectors.

Each node has nine degrees of freedom, thus a two-node linear beam element has 18 degrees of freedom.

A flexible beam element is geometrically described using a position vector $r^{(i)}$ and two slope vectors $r_{\eta}^{(i)}$ and $r_{\zeta}^{(i)}$ for each i -th node (Fig. 6).

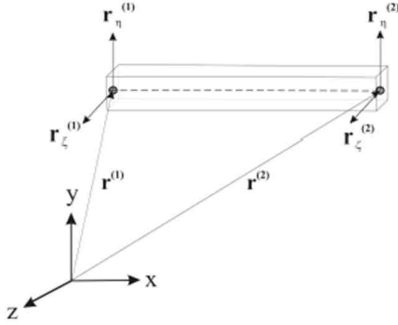


Fig. 6 – Geometrical description of a flexible beam

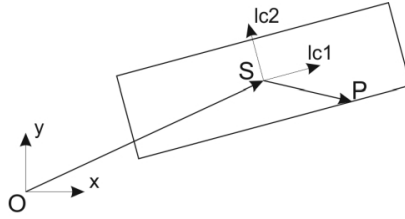


Fig. 7 – Local and global reference frames for a rigid element

The hinge assembly in a simplified form is shown in fig. 5. Aluminum hinge assemblies are modeled as four rotation joints connected by ordinary rigid elements (Fig. 7). Although the real geometry of these assemblies has a different shape (Fig. 4), this representation is justified, since these units have a much greater stiffness than the rod elements of the structure, and their stress-strain state is not under study. The main modeled properties of these hinge assemblies are the stiffness, location, and direction of the rotation axes of the hinges.

In Fig. 7, the letter S denotes the center of mass of the rigid element, which is determined by the position vector in the global reference frame (GRF). The center of mass is also the origin of the local reference frame (LRF). For example, the LRF is used to determine the position of point P in Fig. 7, which is required for adding hinges or sensors.

Additional point masses were used to make the mass of the simplified model of the antenna to be equal to the mass of the real structure. The point masses are determined by three position coordinates.

The hinge of the V-folding bar is modeled by an adjustable universal joint. This joint connects two bodies (hereafter bodies i and bodies j) and makes it possible to constrain six relative degrees of freedom, namely the motion along three axes of the LRF and rotation around these axes. The equations of kinematic constraints for this type of joint have the following form:

$$A^T (x^i - x^j) = 0, \quad (2)$$

where x_1 and x_2 are the positions of the connection points in the GRF on the bodies i and j , respectively; $A = (e_x^i \ e_y^i \ e_z^i)$ is the rotation matrix from the LRF of the joint to the GRF

Each equation in the system (2) corresponds to a constrained direction, so if all directions are constrained, it simplifies as follows:

$$x_i - x_j = \mathbf{0}. \quad (3)$$

If all rotational degrees of freedom are constrained, then the equation of rotational constraints for bodies i and bodies j has the following form:

$$\begin{pmatrix} e_y^j \cdot e_z^i \\ e_x^j \cdot e_z^i \\ e_x^j \cdot e_y^i \end{pmatrix} = \begin{pmatrix} \mathbf{0} \\ \mathbf{0} \\ \mathbf{0} \end{pmatrix}. \quad (4)$$

For the cases when the rotation is not constrained around one of the axes, equation (4) takes the following form:

$$\begin{pmatrix} e_x^j \cdot e_z^i \\ e_x^j \cdot e_y^i \end{pmatrix} = \begin{pmatrix} \mathbf{0} \\ \mathbf{0} \end{pmatrix}, \begin{pmatrix} e_y^j \cdot e_z^i \\ e_y^j \cdot e_x^i \end{pmatrix} = \begin{pmatrix} \mathbf{0} \\ \mathbf{0} \end{pmatrix}, \begin{pmatrix} e_z^j \cdot e_y^i \\ e_z^j \cdot e_x^i \end{pmatrix} = \begin{pmatrix} \mathbf{0} \\ \mathbf{0} \end{pmatrix} \quad (5)$$

for axis x , y , z , respectively.

The diagonal beams are connected through a rotation joint, which constrains all relative degrees of freedom between the two bodies except for rotation about one local axis. A rotation joint is equivalent to a universal joint in which all degrees of freedom are constrained except for rotation around the local x -axis. Also, the rotation joint is used to connect horizontal and diagonal beams to the hinge assemblies.

Rigid bodies are connected by means of a fixed joint that constrains all degrees of freedom of the element in a defined local position. A fixed joint is equivalent to a universal joint, all degrees of freedom of which is constrained.

The antenna is fixed to the boom, which is modeled by the same flexible beam element as the rods of the antenna sections, but with a larger diameter and cross-section. The boom is a vertical beam, which is connected to the hinge assemblies of the first and eighteenth sections of the antenna ring using a rigid hinge at the upper point and a sliding joint at the lower point. The sliding joint ensures that a chosen point of one body moves along the longitudinal axis of the second body. The vector of degrees of freedom of the sliding joint (6) contains the sliding parameter, its time derivative, and the vector of Lagrange parameters. The first three parameters of the Lagrangian represent the sliding forces in the GRF, and the last three parameters are the sliding torques about the axes of the GRF.

$$q = [s \ \dot{s} \ \lambda_1 \ \lambda_2 \ \lambda_3 \ \lambda_4 \ \lambda_5 \ \lambda_6]. \quad (6)$$

Position vectors have the following form:

$$x^i = [x_1^i \ x_2^i \ x_3^i]^T, \quad x^j = [x_1^j \ x_2^j \ x_3^j]^T. \quad (7)$$

where $x_1^{i(j)}$, $x_2^{i(j)}$, $x_3^{i(j)}$ are the three coordinates of the vectors $x^{i(j)}$.

During initialization, the unit vectors of the GRF are transferred to the LRF of each body, thus vectors for the first body v_1^i, v_2^i, v_3^i and for the second body v_1^j, v_2^j, v_3^j are obtained. Equations of displacement and acceleration constraints, respectively (8) have the following form:

$$\begin{bmatrix} r^i(x^i) - r^j(x^j) \\ \frac{\partial r^j(x^j)}{\partial x_1^j} \lambda \\ v_2^j v_3^i \\ v_3^j v_1^i \\ v_2^j v_1^i \end{bmatrix} = \mathbf{0}, \quad \begin{bmatrix} \frac{\partial r^i(x^i)}{\partial t} - \frac{\partial r^j(x^j)}{\partial t} - \frac{\partial r^j(x^j)}{\partial x_1^j} \dot{s} \\ \frac{\partial r^j(x^j)}{\partial x_1^j} \lambda \\ v_2^j v_3^i + v_2^i v_3^j \\ v_3^j v_1^i + v_3^i v_1^j \\ v_2^j v_1^i + v_2^i v_1^j \end{bmatrix} = \mathbf{0}. \quad (8)$$

Modeling antenna nets by flexible beam elements leads to high computation complexity. Because of that the tension effect due to the stretched nets are modeled with the help of springs. The spring elongation is given as follows (9):

$$\Delta x = (\mathbf{p}^{(1)} - \mathbf{p}^{(2)})^T \bar{\mathbf{d}} - l_0, \quad (9)$$

where l_0 is the spring length; $\mathbf{p}^{(1)} = [p_x^{(1)} \ p_y^{(1)} \ p_z^{(1)}]^T$ and $\mathbf{p}^{(2)} = [p_x^{(2)} \ p_y^{(2)} \ p_z^{(2)}]^T$ is the coordinates of the attachment points of the ends of the spring; $\bar{\mathbf{d}}$ is the direction vector, which is defined as follows:

$$\bar{\mathbf{d}} = \frac{\mathbf{p}^{(1)} - \mathbf{p}^{(2)}}{\sqrt{(p_x^{(1)} - p_x^{(2)})^2 + (p_y^{(1)} - p_y^{(2)})^2 + (p_z^{(1)} - p_z^{(2)})^2}}. \quad (10)$$

The resulting spring force is determined as follows:

$$\mathbf{f} = k\Delta x + d\mathbf{v}, \quad (11)$$

where d is the damping ratio; $\mathbf{v} = (\dot{\mathbf{p}}^{(1)} - \dot{\mathbf{p}}^{(2)})^T \bar{\mathbf{d}}$ is the spring velocity; $\dot{\mathbf{p}}^{(1)} = [\dot{p}_x^{(1)} \ \dot{p}_y^{(1)} \ \dot{p}_z^{(1)}]^T$, $\dot{\mathbf{p}}^{(2)} = [\dot{p}_x^{(2)} \ \dot{p}_y^{(2)} \ \dot{p}_z^{(2)}]^T$ are the point velocities.

The deployment cable is not modeled as an independent object. Instead, the forces with which the cable acts on the corresponding pulleys of the inter-sectional hinge assemblies and of the V-bar joints are determined. Cable-driven deployments are modeled as loads acting on the corresponding elements in defined local positions.

Computer model. Currently, the most advanced open source tools for modeling the dynamics of the multibody system are the following software: MBDyn [12], HotInt [13], and FreeDyn [20]. HotInt has been chosen among this software to simulate the antenna deployment because only this tool uses the ANCF methodology.

The antenna modeling process begins with the creation of text script files using Hotint software commands. The structure materials are set in the main script file of the project. The model of each section of the antenna is specified in a separate script file. All files are connected to the main file using the Include command.

The code for each section consists of separate blocks that describe model elements and is created according to the algorithm described below.

First, we set the parameters of cross-sections of the beams and the coordinates of each node of the structure.

To model a flexible beam, we need to define two slope vectors $r_{\eta}^{(k)}$ and $r_{\zeta}^{(k)}$, where $k = 1..18$ is the section number. In the case of a horizontal beam of the ring, the first slope vector is the same for all sections, because it is parallel to the Z axis of the GRF and is equal to the unit vector with coordinates $r_{\eta}^{(k)} = [0; 0; 1]$. The second slope vector, which is perpendicular to the plane of the section, can be found as the vector product as follows:

$$r^{(k)} = (R_1^{(k)} - R_2^{(k)}) \times (R_1^{(k)} - R_3^{(k)}), \quad (12)$$

where $R_1^{(k)}$ is the coordinates of the first node of the horizontal upper beam of the k -th section; $R_2^{(k)}$ is the coordinates of the third node of the horizontal upper beam of the k -th section; $R_3^{(k)}$ is the coordinates of the third node of the horizontal lower beam of the k -th section. Since the slope vector must be a unit vector, we normalize vector (12) as follows:

$$r_{\zeta}^{(k)} = \begin{pmatrix} \frac{r_x^{(k)}}{\|r^{(k)}\|_2} & \frac{r_y^{(k)}}{\|r^{(k)}\|_2} & \frac{r_z^{(k)}}{\|r^{(k)}\|_2} \end{pmatrix}, \quad (13)$$

where $\|r^{(k)}\|_2$ is the Euclidean norm of the vector $r^{(k)}$; $r_x^{(k)}$; $r_y^{(k)}$; $r_z^{(k)}$ is the coordinates of the vector $r^{(k)}$.

Two slope vectors are also required to model a diagonal beam. The first slope of a diagonal beam is equal to the vector (13), and the second one is also determined through the vector product as

$$d^{(k)} = (D_1^{(k)} - D_2^{(k)}) \times (D_1^{(k)} - D_3^{(k)}), \quad (14)$$

where $D_1^{(k)} = R_1^{(k)}$ is the coordinates of the first node of the horizontal upper beam of the k -th section; $D_2^{(k)} = R_3^{(k)}$ is the coordinates of the third node of the horizontal lower beam of the k -th section; $D_3^{(k)} = D_2^{(k)} + r_{\zeta}^{(k)}$.

The coordinates of the slope vector for the diagonal beam of the k -th section are determined by normalizing the vector (14):

$$r_{\eta}^{(k)} = \begin{pmatrix} \frac{d_x^{(k)}}{\|d^{(k)}\|_2} & \frac{d_y^{(k)}}{\|d^{(k)}\|_2} & \frac{d_z^{(k)}}{\|d^{(k)}\|_2} \end{pmatrix}, \quad (15)$$

where $\|d^{(k)}\|_2$ is the Euclidean norm of the vector $d^{(k)}$; $d_x^{(k)}$; $d_y^{(k)}$; $d_z^{(k)}$ is the coordinates of the vector $d^{(k)}$.

The nodes of a flexible beam are created using these slope vectors (13), (15), and the position coordinates of its ends. An example of code for creating nodes and the subsequent creation of a rod is given in the Appendix.

The coordinates of the center of mass and the orientation angles need to be specified to create a rigid body. Only the position coordinates and the mass parameter itself are required to specify a point mass.

To create a rotation joint or universal joint, the rotation axis needs to be specified. A fixed joint does not have such a parameter. For any joints, it is always necessary to determine which two elements are connected, as well as the location of the joint in the LCF of each connecting element. Determining the position of the joint in the LCF is necessary because the elements will be connected precisely at the points where the hinge is located.

A spring can be created by setting up its length, stiffness, and damping, and specifying two elements that will be connected. An example of code for creating a spring is given in the Appendix.

Control elements are used to control the deployment or compression of the antenna. Actuation loads are set up by determining the direction of a load and the local position of the element to which the load is applied. If the load needs to be varied during the deployment process, then the load calculation block needs to be created earlier. Loads are then applied to the selected elements using a HotInt command.

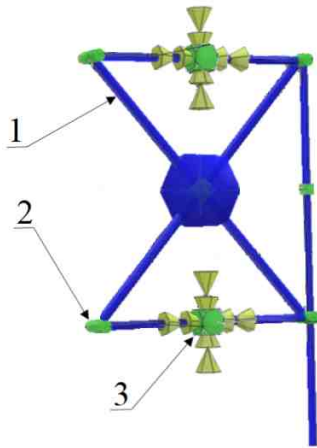


Fig. 8 – HotInt model of the first

springs tightening these sections.

Each created element of the model is represented by a certain set of equations, which is determined by the type of the particular element. As a result of model building, the HotInt forms a system of differential and algebraic equations. The equation of the antenna dynamics can be given in a general form as follows:

$$M(X,t)\ddot{X} + D(X,\dot{X},T) + C(X,t) + \Phi_X \Lambda = V(t), \quad (16)$$

$$\Phi(X) = 0, \quad (17)$$

where $M(X,t)$ is the mass matrix; $D(X,\dot{X},T)$ is the damping vector term; $C(X,t)$ is the stiffness vector term; $V(t)$ is the vector of actuation forces;

To obtain the results of the calculations, it is necessary to create sensors that measure the necessary values. To do this, we need to specify the elements from which the data will be read and select the parameters that need to be measured. An example of code for creating a sensor that measures spring elongation is given in the Appendix.

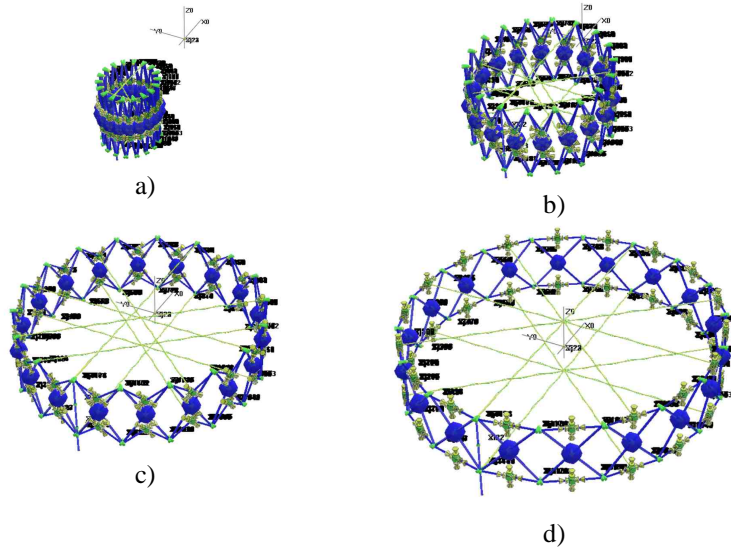
Figure 8 shows the first section of the reflector and the LCF axes of each element in the HotInt. In this figure, the numbers indicate the following: 1 is the flexible beam element, 2 is the rotation joint, 3 is the universal joint.

Figure 9 demonstrates the HotInt model of the full antenna of eighteen sections with

$\Phi(X)$ is the kinematic constraints; Φ_X is the matrix Jacobian of constraints; Λ is the vector of Lagrange multipliers.

The Hotint numerically solves equations (16), (17) using its internal numerical integration tool (solver). The model is integrated using implicit Runge-Kutta schemes. The various Runge-Kutta schemes are implemented by tables of coefficients defined by files that are automatically generated by built-in functions.

To start simulating the antenna deployment using the built model, it is necessary to obtain the initial conditions. These conditions are the state vector of the antenna in the stowed state and are obtained by applying uniform loads to the points between the horizontal beams of each section to compress the antenna ring to the required stowed state. The initial, intermediate, and final states of the antenna during the simulation of its deployment are shown in fig. 9.



a – stowed antenna; b – stage 1 of the antenna deployment; c – stage 2 of the antenna deployment; d – deployed antenna.

Fig. 9 – States of the antenna deployment

To deploy the antenna from the obtained stowed state, the same uniform loads were applied to the same nodes, but in the opposite direction.

System data and simulation results. This section presents the simulation results of the antenna deployment, which differs in applied actuation forces, namely: case 1 – 0.015 N, case 2 – 0.02 N, and case 3 – 0.03 N.

The initial data given in Table 1 were used for simulation of the antenna deployment.

Table 1. Parameters of the antenna.

Parameter	Value	Units
Semi-major axis of the antenna ellipse	3.5184	m
Minor axis of the ellipse of the antenna	3.2856	m
Antenna section height	0.63	m
Length of the diagonal rod	0.4275	m
Outer diameter of the diagonal rod	0.01	m
Inner diameter of the diagonal rod	0.00915	m
Length of the horizontal rod	0.2889	m
Outer diameter of the horizontal rod	0.012	m
Inner diameter of the horizontal rod	0.01115	m
Length of the boom rod	0.2889	m
Outer diameter of the boom rod	0.06	m
Inner diameter of the boom rod	0.058	m
Young's modulus of the rods	120	GPa
Rod density	1800	kg/m ³
Poisson's ratio of the rods	0.3	-
Damping ratio of the rod	0.001	-
Density of the rigid bodies	13975.49 7	kg/m ³
Point mass	0.0198	kg
Spring stiffness	0.001	N/m
Damping ratio of the spring	0.01	Nm/s ²
Neutral length the spring	0.7116	m

According to the simulation results, the antenna reached its final deployed state in 17.58 sec, 15.06 sec, and 12.16 sec, for cases 1, 2, 3, respectively. Figure 10 shows the variations of the angles between the V-folding bars of the first section during the antenna deployment. Stress variations in the diagonal beams during the antenna deployment are plotted in Figs. 11 – 13 by the black and red lines for the first and ninth sections, respectively.

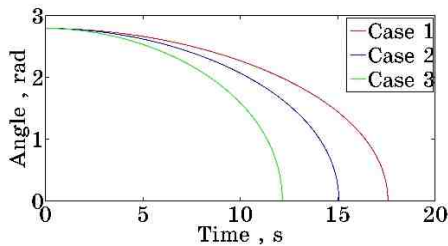


Fig. 10 – Variations of the angles between the V-folding bars

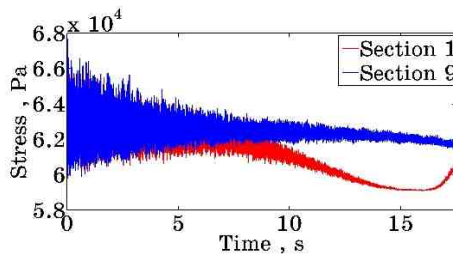


Fig. 11 – Stress variations in the diagonal beams (Case 1)

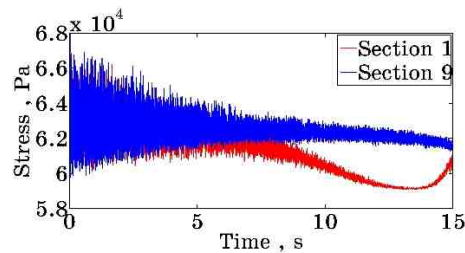


Fig. 12 – Stress variations in the diagonal beams (Case 2)

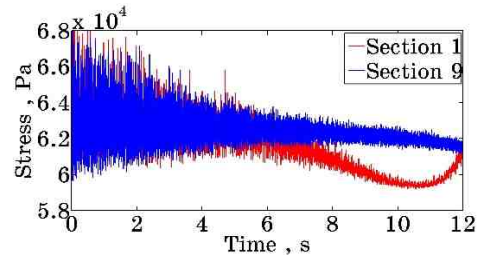


Fig. 13 – Stress variations in the diagonal beams (Case 2)

Conclusion. The article presents the methodology that allows open source software to be applied for modeling a space reflector antenna. A model of the antenna is designed for simulating the deployment processes. The reflector deployment is simulated using various values of the deploying forces and the variations of the main parameters of the antenna on time were obtained. The model uses a simplified representation of the cable deployment system, so more detailed modeling of this system may be the subject of research in the future.

1. Khoroshylov S., Shamakhanov V., Vasylyev V. Modeling of centrifugal deployment of three-section minisatellite boom. *Teh. Meh.* 2021. No. 4. Pp. 56–65. <https://doi.org/10.15407/itm2021.04.056>
2. Alpatov A., Gusynin V., Belonozhko P. *et.al.* Shape control of large reflecting structures in space. 62nd International Astronautical Congress, 3–7 October, Cape Town, South Africa, 2011. Pp. 5642–5648.
3. Alpatov A., Gusynin V., Belonozhko P., Khoroshylov S., Fokov A. Configuration modeling of cable-stayed space reflectors. *Proceedings of the 64nd International Astronautical Congress.* Beijing, China, 2013. Pp. 5793–5799.
4. Duan B., Zhang Y., Du J. *Large Deployable Satellite Antennas: Design Theory, Methods and Applications* Springer Nature, 2020. 271 pp. <https://doi.org/10.1007/978-981-15-6033-0>
5. Mitsugi J., Ando K., Senbokuya Y., Meguro A. Deployment analysis of large space antenna using flexible multibody dynamic simulation. *Acta Astronautica.* 1990. V.47. No.1. Pp. 19–26. [https://doi.org/10.1016/S0094-5765\(00\)00014-X](https://doi.org/10.1016/S0094-5765(00)00014-X)
6. Tsunoda H., Miyoshi K. Deployment test methods for a large deployable mesh reflector. *Journal of Spacecraft and Rockets.* 1997. V.34. No.6. Pp. 811–816. <https://doi.org/10.2514/2.3291>
7. Li T.J., Zhang Y., Li T., Deployment dynamic analysis and control of hoop truss deployable antenna. *Acta Aeronautica et Astronautica Sinica.* 2009. V. 30. No.3. Pp. 444–449.
8. Li T. J. Deployment analysis and control of deployable space antenna. *Aerosp. Sci. Technol.* 2012. V.18. No.1. Pp. 42–47. <https://doi.org/10.1016/j.ast.2011.04.001>
9. Zhangn Y., Duan B., Li T. J. A controlled deployment method for flexible deployable space antennas. *Acta Astronautica.* 2012. V. 81. No.1. Pp.19–29. <https://doi.org/10.1016/j.actaastro.2012.05.033>
10. Sushko O., Medzmariashvili E., Tserodze S. *et al.* Design and analysis of light-weight deployable mesh reflector antenna for small multibeam SAR satellite, EUSAR 2021: Proceedings of the European Conference on Synthetic Aperture Radar, 29 March – 01 April 2021. Pp. 421–423.
11. Sushko O., Medzmariashvili E., Filipenko F. *et al.* Modified design of the deployable mesh reflector antenna for mini satellites. *CEAS Space J.* 2011. V.13. No.4. Pp. 533–542. <https://doi.org/10.1007/s12567-020-00346-0>
12. Masarati P., Morandini M., Quaranta G., Mantegazza P. Computational aspects and recent improvements in the open-source multibody analysis software “MBDyn”. *ECCOMAS Thematic Conference.* 2005. V.4. 1895024.
13. Gerstmayr J., Dorninger A., Eder R. *et al.* HOTINT: A Script Language Based Framework for the Simulation of Multibody Dynamics Systems. *ASME IDETC/CIE.* 2013. V. 7B. V07BT10A047. <https://doi.org/10.1115/DETC2013-12299>
14. Fraux V., Lawton M., Reveles J. R., You Z. Novel large deployable antenna backing structure concepts for foldable reflectors. *CEAS Space J.* 2013. V.5. Pp.195–201. <https://doi.org/10.1007/s12567-013-0046-5>
15. Mikulas M.M., Collins T. J., Hedgepeth J. M. Preliminary design approach for large high precision segmented reflectors. *NASA Technical Memorandum* 102605. 1990. Pp. 1–51.
16. Miura K., Miyazaki Y., Concept of the tension truss antenna. *AIAA Journal.* 1990. V. 28. Pp.1098–1202. <https://doi.org/10.2514/3.25172>

17. Thomson M. W. The Astromesh deployable reflector. IEEE Trans. on Antennas and Propagation. 1990. V. 3. Pp. 1516–1535.
18. Sun J., Tian Q., Hu H., Pedersen N. Axially variable-length solid element of absolute nodal coordinate formulation. Acta Mechanica Sinica. 2019. V. 35. Pp. 653–663. <https://doi.org/10.1007/s10409-018-0823-7>
19. Sautter K., Meßmer M., Teschemacher T., Bletzinger K. Limitations of the St. Venant-Kirchhoff material model in large strain regimes. International Journal of Non-Linear Mechanics. 2022. V. 147. 104207. <https://doi.org/10.1016/j.ijnonlinmec.2022.104207>
20. Nachbagaer K., Sherif K., Witteveen W., FreeDyn – A multibody simulation research code. Proceedings of the 11th World Congress on Computational Mechanics (WCCM) and the 5th European Conference on Computational Mechanics (ECCM). 2014. Pp. 49–53.

Received on October 13, 2022
in final form on November 21, 2022